Effect of Penetrant−Polymer Interactions on Molecular Diffusion in Conformational Isomers of a Heterogeneous Polymer

Yossef A. Elabd,[†] James M. Sloan,[‡] Nora Beck Tan,[‡] and Timothy A. Barbari*[,§]

Department of Chemical Engineering, Johns Hopkins University, Baltimore, Maryland 21218; U.S. Army Research Laboratory, Aberdeen Proving Ground, Maryland 21005; and Department of Chemical Engineering, University of Maryland, College Park, Maryland 20742

Received December 11, 2000; Revised Manuscript Received June 18, 2001

ABSTRACT: The diffusion of deuterated hexane in conformational isomers of a heterogeneous polymer, H_{12}MDI (4,4′-dicyclohexylmethane diisocyanate)/BD (1,4-butanediol)/PTMO (poly(tetramethylene oxide)), was investigated at a fixed hard segment content of 30 wt % and compared to the diffusion of acetonitrile. The effective diffusion coefficient of acetonitrile decreases with increasing trans−trans isomer content while that for deuterated hexane remains constant. These results suggest that the trend observed from acetonitrile diffusion is a function of penetrant−polymer interactions and not tortuosity effects. A model with penetrant−polymer binding to the surface of the dispersed hard segment domains of the heterogeneous polymer was developed to elucidate the main factors contributing to the interaction or hindrance effect, which were determined to be the "available" surface binding sites and the surface-to-volume ratio of the hard segment domains. FTIR-ATR spectroscopy was used to quantify this interaction effect, and SAXS was used to confirm the findings.

Introduction

In a recent study,[1] the diffusion of acetonitrile in conformational isomers of a phase-segregated (heterogeneous) polyurethane, H_{12}MDI (4,4′-dicyclohexyl methane diisocyanate)/BD (1,4-butanediol)/PTMO (poly(tetramethylene oxide)), was investigated at a fixed hard segment content of 30 wt %, using FTIR-ATR spectroscopy. Typically in polyurethanes at low hard segment weight fractions, the hard segments hydrogen bond to each other (NH- - -O═C) and form dispersed domains within a soft segment continuum. For this particular polyurethane, the conformational isomers of the hard segment (H_{12}MDI) exist as three separate isomers: cis−cis, cis−trans, and trans−trans, shown in Figure 1, which hydrogen bond to one another to form amorphous domains. Samples with higher trans−trans content revealed increased hydrogen bonding between hard segments and a lower effective diffusion coefficient for acetonitrile.[1] In addition, the infrared revealed changes in the C═O and NH spectra in the hard segment of the polymer and the C≡N spectra of the penetrant, elucidating hydrogen bonding between penetrant and polymer. The trend observed for the effective diffusion coefficient was attributed to both penetrant−polymer interactions and changing tortuosity, due to the changing morphology among the different polyurethane isomers.

Diffusion in a heterogeneous system without penetrant−polymer interactions has been explored by many investigators.[2−20] In one of the earliest and best known studies,[2] Maxwell examined diffusion in a heterogeneous material containing nonoverlapping spherical inclusions randomly placed throughout the material. The resulting equation is expressed as

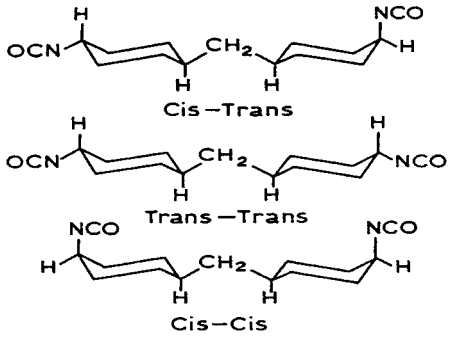

Figure 1. H_{12}MDI conformational isomers.

$$\frac{D_{\text{eff}}}{D_A} = \frac{2D_A + D_B - 2\phi(D_A - D_B)}{2D_A + D_B + \phi(D_A - D_B)} \tag{1}$$

where D_{eff} is the effective or overall diffusion coefficient of the penetrant in the entire system and D_A and D_B are the penetrant diffusivities in the continuous and dispersed phases, respectively. ϕ is the volume fraction of the dispersed phase. When the dispersed phase is impermeable ($D_B = 0$), eq 1 reduces to

$$\frac{D_{\text{eff}}}{D_A} = \frac{2(1-\phi)}{2+\phi} \tag{2}$$

Interestingly, Maxwell's equation reveals that the ratio of the diffusivities is simply a function of the volume fraction of the dispersed phase. Since this study, other investigators[3−7] have derived different equations for the problem of dispersed spheres, but all have arrived at a similar conclusion: the ratio of the diffusivities is only a function of volume fraction. A more recent study[8] has shown, through Monte Carlo simula-

[†] Johns Hopkins University.
[‡] U.S. Army Research Laboratory.
[§] University of Maryland.
* To whom correspondence should be addressed: phone 301-405-2983; Fax 301-405-0523; e-mail barbari@eng.umd.edu.

10.1021/ma002107c CCC: $20.00
Published on Web 07/26/2001

tions, that the spatial arrangement of dispersed spheres has no effect on the diffusivity at constant volume fraction. In addition, Fricke[9] concluded, for spheriods suspended in a continuum, that the diffusivities are independent of the size of the suspended particles at constant volume fraction. Hamilton and Crossover[10] extended Fricke's model to ellipsoids and found that shape has a negligible effect on the diffusivity. Cheng and Vachon[11] extended the work of Tsao[12] to randomly dispersed particles of irregular shape and size and showed that the diffusivities depend only on volume fraction. Numerical solutions by Bell and Crank[13] for rectangular blocks and Keller and Sacks[14] for uniform cylinders both revealed that the diffusivity is related to the width and radii, respectively, of the dispersed phase which are both proportional to volume fraction.

Diffusion in semicrystalline polymers has also been investigated[15,16] and can be described as a heterogeneous system, in which the penetrant diffuses through the amorphous regions and is altered in its path by impermeable crystalline regions. The effective diffusion coefficient in this system is commonly expressed by

$$\frac{D_{\text{eff}}}{D_{\text{A}}} = \frac{1}{\beta\tau} \tag{3}$$

where β is the constriction factor, which is related to the mobility of the amorphous chains, and τ is the tortuosity, which is a structure-dependent parameter related to the altered path of a penetrant due to the inhomogeneous nature of the diffusing medium. In addition, diffusion in porous solids, which is analogous to this problem, is traditionally represented by

$$\frac{D_{\text{eff}}}{D_{\text{A}}} = \frac{\epsilon}{\tau} = \frac{1-\phi}{\tau} \tag{4}$$

where ϵ is the void volume or the volume fraction of the continuous phase. Relationships for tortuosity have been derived in many studies,[17−20] which show this parameter is a function only of volume fraction. All of these studies suggest that the tortuosity will remain constant at a fixed volume fraction in a heterogeneous system, even if the size and shape of the dispersed phase change.

In the present study, the model predictions were explored experimentally (FTIR-ATR spectroscopy) by studying the diffusion of dueterated hexane, a noninteracting penetrant, in conformational isomers of a heterogeneous polyurethane, H_{12}MDI (4,4′-dicyclohexylmethane diisocyanate)/BD (1,4-butanediol)/PTMO (poly(tetramethylene oxide)), where the size and arrangement of the dispersed phase changes (H_{12}MDI isomers) but the volume fraction remains constant. A comparison between these results and those from a previous study[1] for the diffusion of acetonitrile provides insight into the effect of penetrant−polymer interactions on the overall transport rate in a heterogeneous system. A transport model incorporating penetrant−polymer interactions to hard segments in a heterogeneous polymer was developed to elucidate the main factors contributing to the diffusion of acetonitrile. FTIR-ATR spectroscopy was used to quantify these factors, and the approach here is similar to a study conducted by Elabd and Barbari[21] where penetrant−polymer interactions were quantified in a homogeneous polymer using this same experimental technique. Small-angle X-ray scattering (SAXS) was used to complement the transport model and FTIR-ATR experiments, exploring morphological differences among the isomers.

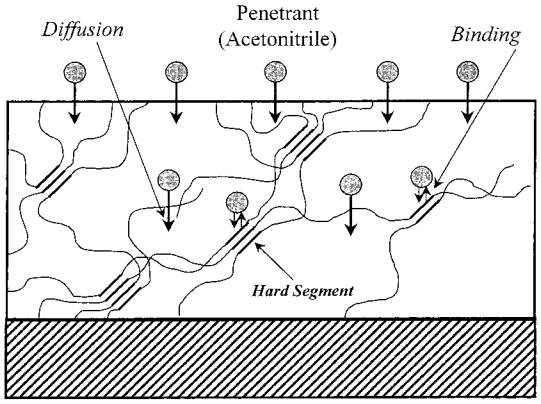

Figure 2. Schematic depicting acetonitrile diffusion through the soft segment of a polyurethane with hydrogen-bonding interactions with the surface binding sites of the hard segment domains. Hydrogen-bonding interactions hinder the diffusion process.

Model Development

Figure 2 is a schematic representation of the diffusion process in a heterogeneous polyurethane with hard segments at a low volume fraction and with binding to their domain surfaces. The interacting penetrant, acetonitrile, diffuses through the soft segment (PTMO) and interacts through hydrogen bonding to hard segment (H_{12}MDI) binding sites (NH) on the surface of these dispersed domains. The H_{12}MDI hard segment domains are glassy and amorphous.

To describe this process mathematically, a diffusion model with a reversible binding reaction was developed. The reaction between penetrant and binding site can be written as

$$\text{A} + \text{B} \underset{k_{\text{r}}}{\overset{k_{\text{f}}}{\rightleftharpoons}} \text{AB} \tag{5}$$

where A, B, and AB represent the free penetrant (acetonitrile), the polymer binding site (NH), and the hydrogen-bound acetonitrile complex, respectively. k_{f} and k_{r} represent the forward and reverse rate constants, respectively. The one-dimensional continuity equation for species A in a heterogeneous film is

$$(1-\phi)\frac{\partial C_{\text{A}}}{\partial t} = D_{\text{eff}}\frac{\partial^2 C_{\text{A}}}{\partial z^2} + \phi\eta r_{\text{A}} \tag{6}$$

where z corresponds to the distance in the film, t represents time, C_{A} is the concentration of A (free acetonitrile), and η is the surface area-to-volume ratio of dispersed hard segment domains. D_{eff} is the effective diffusion coefficient of the diffusing or free penetrant. For a fixed number of available binding sites, q_{B}^0 (surface concentration or moles per area), the rate of binding can be described by a Langmuir expression:

$$-r_{\text{A}} = k_{\text{f}} C_{\text{A}} q_{\text{B}}^0 (1-\theta) - k_{\text{r}} q_{\text{B}}^0 \theta \tag{7}$$

where θ is the fraction of occupied sites, $q_{\text{AB}}/q_{\text{B}}^0$. The

corresponding equation for hydrogen-bound acetonitrile is

$$\frac{\partial q_{AB}}{\partial t} = q_B^0 \frac{\partial \theta}{\partial t} = -r_A \tag{8}$$

Adding eqs 6 and 8 gives

$$(1-\phi)\frac{\partial C_A}{\partial t} = D_{eff}\frac{\partial^2 C_A}{\partial z^2} - \phi\eta q_B^0 \frac{\partial \theta}{\partial t} \tag{9}$$

If local equilibrium is assumed, an equilibrium constant can be written in terms of the concentrations of each species as

$$K = \frac{q_B^0 \theta}{C_A q_B^0 (1-\theta)} \tag{10}$$

At low penetrant concentrations, the binding sites never reach saturation ($\theta \ll 1$), and eq 10 reduces to

$$q_B^0 K = \frac{q_{AB}}{C_A} \tag{11}$$

By combining eqs 9 and 11, the continuity equation can be written in terms of C_A only:

$$\frac{\partial C_A}{\partial t} = \left(\frac{D_{eff}}{(1-\phi)+\phi\eta q_B^0 K}\right)\frac{\partial^2 C_A}{\partial z^2} \tag{12}$$

Equation 12 can also be written exclusively in terms of C_T, the total concentration of acetonitrile (free and hydrogen bound):

$$\frac{\partial C_T}{\partial t} = \left(\frac{D_{eff}}{(1-\phi)+\phi\eta q_B^0 K}\right)\frac{\partial^2 C_T}{\partial z^2} \tag{13}$$

Equation 13 can be used with the total concentration or absorbance of acetonitrile that was measured in the previous study.[1] Equations 12 and 13 describe the transport of acetonitrile in terms of a new effective diffusion coefficient, which includes the effect of interactions between penetrant and polymer:

$$D^*_{eff} = \left(\frac{D_{eff}}{(1-\phi)+\phi\eta q_B^0 K}\right) \tag{14}$$

In eq 14, penetrant−polymer interactions hinder diffusion by the factor $(1-\phi)+\phi\eta q_B^0 K$.

Alternatively, the model could have been developed with a bulk equilibrium binding term in place of the surface binding term in eq 6. The same general form results for eq 14 with ηq_B^0 replaced with the bulk concentration of binding sites in the hard segments, C_B^0. This approach is similar to a previous study in which the penetrant interacted with homogeneously distributed binding sites.[21] However, other studies have experimentally shown that H_{12}MDI hard segment domains are impermeable to a variety of penetrants.[22,23] Therefore, acetonitrile interactions with the hard segment domains were treated as an adsorption process.

Table 1. H_{12}MDI/BD/PTMO 2000 Conformational Isomer Samples and Their Densities

sample	% cis−cis	% cis−trans	% trans−trans	density (g/cm^3)
I	10	61	29	1.08
II	1	9	90	1.05

Table 2. H_{12}MDI/BD/PTMO Conformational Isomer Samples and Their Compositions

sample	trans−trans (%)	PTMO/H_{12}MDI/BD mole ratio	wt %[a] hard segment	(ϕ) vol % hard segment
I	29	1/2.6/1.5	30	22
II	90	1/2.6/1.5	30	24

[a] Hard segment (wt %) = [(moles of H_{12}MDI) × M_{H12MDI} + (moles of BD) × M_{BD}]/[(moles of PTMO) × M_{PTMO} + (moles of H_{12}MDI) × M_{H12MDI} + (moles of BD) × M_{BD}] × 100%, where M_{PTMO} = 1934, M_{H12MDI} = 262, and M_{BD} = 90.

Using FTIR-ATR spectroscopy, the effective diffusion coefficient can be determined from the regression of experimental ATR absorbance to the ATR solution of eq 13:[1]

$$\frac{A_t}{A_{eq}} = 1 - \frac{8}{\pi d_p (1-e^{-2L/d_p})}\sum_{n=0}^{\infty}\frac{e^g[f e^{-2L/d_p} + (-1)^n (2/d_p)]}{(2n+1)(4/d_p^2 + f^2)} \tag{15}$$

where

$$g = \frac{-D_{eff}(2n+1)^2\pi^2 t}{4L^2} \tag{16}$$

$$f = \frac{(2n+1)\pi}{2L} \tag{17}$$

$$d_p = \frac{\lambda}{2n_2\pi\sqrt{\sin^2\theta - \left(\frac{n_1}{n_2}\right)^2}} \tag{18}$$

A_t is the integrated infrared absorbance of the diffusing penetrant at time t, A_{eq} is its value at equilibrium, d_p (eq 17) is the depth of penetration of infrared radiation into the polymer film where n_1 and n_2 are the refractive indices of the polymer and the ATR crystal, respectively, θ is the angle of incidence, and λ is the wavelength of absorbed light.

Experimental Section

Materials and Sample Preparation. Samples of H_{12}MDI /BD/PTMO 2000 polyurethane were supplied and synthesized by the Army Materials and Mechanics Research Center.[24] H_{12}-MDI (4,4′-dicyclohexylmethane diisocyanate) is the hard segment, BD (1,4-butanediol) is a chain extender, and PTMO 2000 (poly(tetramethylene oxide)) (mol wt 2000) is the polyether soft segment. The diisocyanate isomer ratios and properties of the H_{12}MDI/BD/PTMO polyurethane samples used in these experiments are shown in Tables 1 and 2. Details concerning the synthesis and preparation of these samples for FTIR-ATR experiments can be found elsewhere.[1,24] Deuterated hexane was purchased from Aldrich Chemical Co. Inc. (30300-3) with a purity of 99 at. % and was stored under nitrogen.

ATR and Gravimetric Experiments. An FTIR spectrometer (Mattson Research Series 1) with a horizontal ATR cell and a zinc selenide trapezoidal ATR crystal (Graseby Specac,

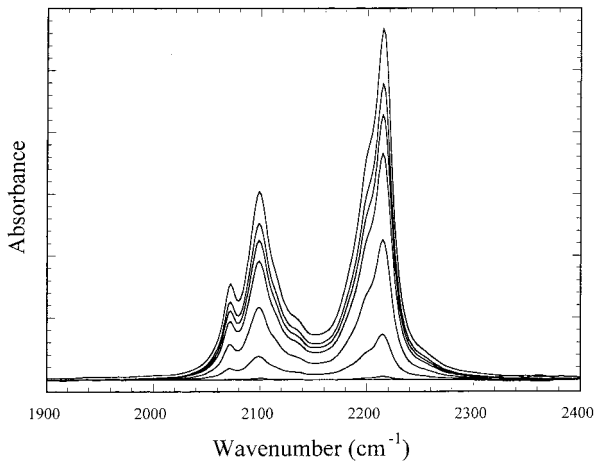

Figure 3. Time-evolved deuterated hexane absorbance spectra in H_{12}MDI/BD/PTMO at 23 °C (90% trans−trans isomer).

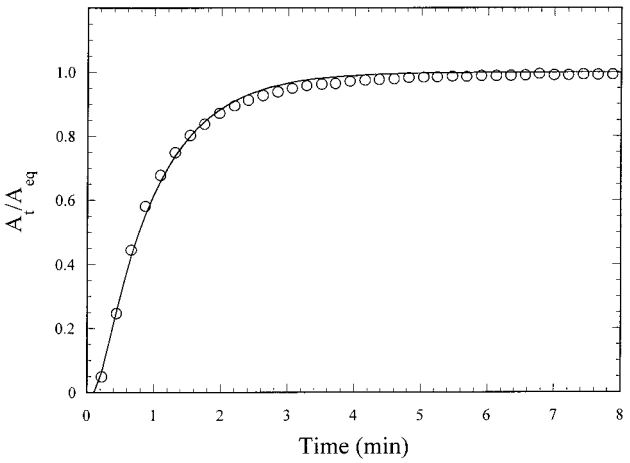

Figure 4. FTIR-ATR data (open symbols) for diffusion of deuterated hexane in H_{12}MDI/BD/PTMO at 23 °C (90% trans−trans isomer) regressed with a Fickian model (solid line).

Inc.) was used to obtain all infrared spectra for the diffusion experiments at 23 ± 1 °C. A conventional quartz spring gravimetric balance was used to obtain weight gain measurements of acetonitrile in the polyurethane samples at a vapor activity of approximately one. For gravimetric experiments, the polyurethane films were prepared similarly to those for the FTIR-ATR experiments but were cast into an aluminum mold and hung directly on the quartz spring. Details regarding the experimental equipment and procedures can be found elswhere.[1,25]

Density Experiments. The density of each H_{12}MDI/BD/PTMO polyurethane sample was measured using a helium pycnometer (Quantachrome Ultrapycnometer 1000), and the results are listed in Table 1. This is a noninvasive procedure using purified helium as the displaced medium. After calibration, the specimens were placed in the measurement cell and purged with helium for 6 min. Fifteen samples were taken for each data point.

SAXS Experiments. Small-angle X-ray scattering (SAXS) was performed on a beamline X27C at the National Synchrotron Light Source, Brookhaven National Laboratory, Upton, NY. Two-dimensional scattering patterns were collected on a pinhole-collimated system using Fujitsu image plates and read by a Fujitsu BAS 2000 image plate reader. Specialty software available at Brookhaven National Laboratory was used to reduce two-dimensional data to one-dimensional intensity vs scattering vector (q) plots after background subtraction by circular averaging. The X-ray wavelength employed was 1.307 Å.

Results and Discussion

Deuterated Hexane Diffusion. To distinguish between penetrant−polymer binding and tortuosity effects between the two isomer samples, the diffusion of deuterated hexane, a noninteracting penetrant, in the H_{12}-MDI polyurethanes was investigated. Time-evolved infrared spectra representing the C−D stretching of deuterated hexane diffusion in the 90% trans−trans isomer of the H_{12}MDI polyurethane (sample II) is shown in Figure 3. Deuterated hexane was chosen instead of hexane because the C−D stretch (2300−2000 cm^{-1}) does not interfere with the C−H stretching of the polyurethane (3000−2700 cm^{-1}). The C−D stretch was integrated at each time point over this wavelength range with a procedure described in a previous study.[1] Figure 4 displays the results of the normalized integration over time with open symbols. The solid line represents the regression to eq 15 for the determination of the effective diffusion coefficient. Table 3 lists the diffusion coefficient of deuterated hexane in both samples, I and II (29% and 90% trans−trans, respectively). The diffusion coefficients are, within experimental error, the same at a fixed hard segment volume fraction. The diffusion coefficients measured for acetonitrile from a previous study[1] are repeated here in Table 3 for comparative purposes. The experimental results for deuterated hexane confirm the theoretical developments discussed above, illustrating that the diffusivities in the absence of binding are a function of only the volume fraction. This suggests that penetrant−polymer interactions are the reason for the large difference observed for acetonitrile with changing polyurethane isomer content (shown in Table 3). It should be noted that acetonitrile is much smaller ($\bar{V}$ = 52.2 cm^3/mol) then deuterated hexane ($\bar{V}$ = 130.8 cm^3/mol) and is expected to have a higher diffusion coefficient.

Table 3. Diffusion Results for Deuterated Hexane and Acetonitrile in H_{12}MDI/BD/PTMO

sample	ϕ	D_{eff}(deuterated hexane) ($\times 10^7$) (cm^2/s)	D^*_{eff}(acetonitrile)[a] ($\times 10^7$) (cm^2/s)
I	0.22	3.4 ± 0.3	13.0 ± 0.7
II	0.24	2.9 ± 0.4	5.2 ± 0.3

[a] Reference 1.

Table 4. NH, C═O, and C≡N Concentrations in H_{12}MDI/BD/PTMO

		hydrogen-bound C═O (%)[a]		
sample	NH (M)	without acetonitrile	with acetonitrile[b]	acetonitrile[b] (M)
I	2.06	59	51	0.74
II	2.01	71	50	0.67

[a] Reference 1. [b] At equilibrium sorption.

Penetrant−Polymer Interactions. From the previous study,[1] hydrogen bonding between the C≡N bond in acetonitrile and the NH bond in the hard segment of the polyurethane was observed through changes in C≡N, NH, and the C═O infrared stretching vibrations. Additional peaks appeared in the C≡N stretch of the penetrant and NH stretch of the polymer hard segments, representing hydrogen bonding between penetrant and polymer. Interestingly, a population shift between the hydrogen-bound and free C═O groups in the hard segments was observed, shown in Table 4. The acetonitrile molecules compete with the NH- - -O═C bond to hydrogen bond to the NH groups on the surface of the hard segment domains, hindering their diffusion

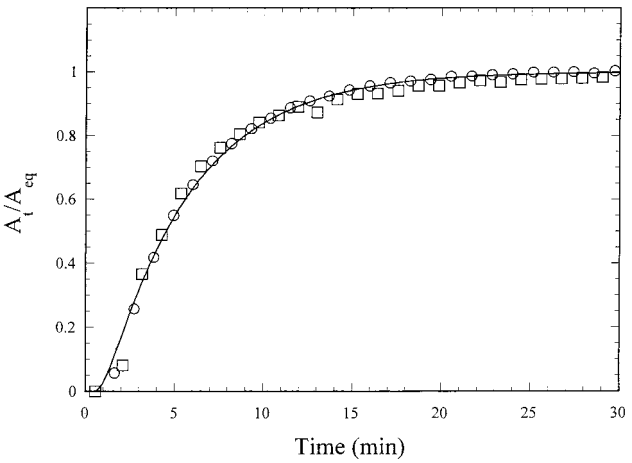

Figure 5. FTIR-ATR data (open symbols) for the diffusion of acetonitrile (circles) and the change in free C═O groups (squares) in H_{12}MDI/BD/PTMO at 23 °C (90% trans−trans isomer). The data were regressed to a Fickian model represented by the solid line.

(NH- - -N≡C). To confirm the assumption of local equilibrium in the model development here, the increase in free C═O groups over the diffusion time was compared to the rate at which acetonitrile increases, shown in Figure 5. The increase in free C═O groups occurs at the same rate as the diffusion of acetonitrile, suggesting that the adsorption or binding between acetonitrile and the polymer is proportional to the change in C═O groups.

Determination of Penetrant−Polymer Interaction Effect. To determine the extent to which diffusion is hindered, $(1 - \phi) + \phi\eta q_B^0 K$ (eq 14), the individual parameters in this expression must be quantified experimentally. The measured concentration of hydrogen-bound acetonitrile (moles/volume of polymer) can be related to the surface concentration (moles/area of dispersed phase), surface area-to-volume ratio, and volume fraction of dispersed phase:

$$C_{AB} = \phi\eta q_{AB} \tag{19}$$

Substituting eq 19 into eq 11 results in

$$\phi\eta q_B^0 K = \frac{C_{AB}}{C_A} \tag{20}$$

From Figure 5, the difference in C═O groups (1:1 ratio to NH groups), ΔC_B, is equivalent to the hydrogen-bound acetonitrile concentration, C_{AB}:

$$\Delta C_B = C_{AB} \tag{21}$$

and is listed in Table 4. This calculation was made using equivalent extinction coefficients for both hydrogen-bound and free carbonyl bands, which has been demonstrated experimentally in a variety of polyurethanes.[26−30] In addition, the concentration of free acetonitrile, C_A, can be determined from eq 21 and experimental data for total acetonitrile concentration, C_T:

$$C_A = C_T - C_{AB} \tag{22}$$

In this study, the total acetonitrile concentration was determined from gravimetric sorption at unit activity, and the results are shown in Table 4. The hindrance factor, $(1 - \phi) + \phi\eta q_B^0 K$, was calculated with the use of eqs 20−22 using equilibrium concentrations, and the results are shown in Table 5. The effect of penetrant−polymer interactions illustrates that the overall transport rate is hindered by a factor of 1.06 for sample I and 2.44 for sample II, corresponding to the differences in hydrogen-bound penetrant in Table 4. The larger hindrance factor for sample II can be attributed to a larger surface area-to-volume ratio of the dispersed phase (η) and consequently more available surface binding sites (q_B^0), since the equilibrium constant (K) and volume fraction (ϕ) are constants for this system. Upon accounting for the interactions, the actual effective diffusion coefficients are, within experimental error, the same, as would be expected at a fixed volume fraction of the dispersed phase, and which was demonstrated with the diffusion of deuterated hexane (Table 3).

Table 5. Penetrant−Polymer Interaction Effects for Acetonitrile in H_{12}MDI/BD/PTMO

sample	D_{eff}^*(acetonitrile)[a] ($\times 10^7$) (cm^2/s)	$\phi\eta q_B^0 K$	$(1-\phi)+\phi\eta q_B^0 K$	D_{eff}(acetonitrile) ($\times 10^7$) (cm^2/s)
I	13.0 ± 0.7	0.28	1.06	13.8 ± 0.7
II	5.2 ± 0.3	1.68	2.44	12.7 ± 0.7

[a] Reference 1.

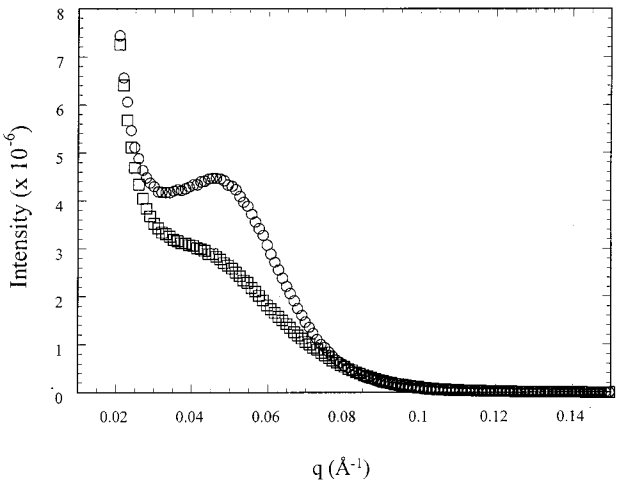

Figure 6. SAXS intensity profile (I vs q) for 29% (circles) and 90% (squares) trans−trans isomer H_{12}MDI/BD/PTMO.

SAXS Data and Analysis. To confirm this variation in morphology between the two different isomers, small-angle X-ray scattering (SAXS) experiments were conducted on both samples. Figure 6 shows intensity profiles (I vs q) for each sample where q is the scattering vector:

$$q = \frac{4\pi \sin(\theta/2)}{\lambda} \tag{23}$$

and θ and λ are the scattering angle and wavelength, respectively. Scattering intensity describes the local heterogeneities in the electron density of the material, and the intensity maxima in Figure 6 (between 0.02 and 0.08 Å^{-1} (q)) are an indication of the microphase separation that occurs. These results are analogous to a study conducted by Van Bogart et al.[31] on H_{12}MDI polyurethanes with varying soft segment molecular weights at a fixed hard segment content. Their study revealed increases in intensity similar to Figure 6, and they calculated an increase in hard segment domain size and a decrease in the surface area-to-volume ratio as

Table 6. SAXS Analysis

sample	trans−trans (%)	q_{max} (Å^{-1})	L (Å)
I	29	0.047	133.6
II	90	0.036	174.5

the soft segment molecular weight increased. In addition, the long spacing, which has been interpreted as the average separation distance of the microdomains, can be calculated from Bragg's law:[32]

$$\lambda = 2L \sin(\theta/2) \tag{24}$$

The long spacing, L, is determined from the maximum in the scattering intensity in Figure 6, and the results are listed in Table 6. These results reveal a smaller separation distance in sample I (29% trans−trans), suggesting larger hard segment domain size and a decrease in the surface area-to-volume ratio. Physically, this may occur because decreasing the trans−trans isomer content results in more steric hindrances[24,33,34] and less ideal packing conditions among the hard segments. This results in fewer hard segment domains of larger size, producing larger surface area-to-volume ratios and fewer "available" surface binding sites. This morphological change agrees well with the transport model and FTIR-ATR experiments.

Conclusions

In this study, the ability of time-resolved FTIR-ATR spectroscopy to quantitatively monitor changes in the molecular state of both the penetrant and the polymer was demonstrated. The technique also provides insight into transport mechanisms in more complicated systems, such as multicomponent or heterogeneous polymer membranes and penetrant−polymer binding to the surface of phase-segregated domains. The transport model developed for penetrant−polymer binding in a heterogeneous polymer reveals that the main factors hindering diffusion are the surface area-to-volume ratio of the dispersed phase and the "available" surface binding sites. These factors were quantified with FTIR-ATR spectroscopy, and when accounted for, the results for the interacting penetrant (acetonitrile) compare well with those obtained from the diffusion of a noninteracting penetrant (deuterated hexane). SAXS results also confirm the observations in this study.

Acknowledgment. The authors acknowledge the financial support of the U.S. Army Research Office through Grant DAAD19-00-1-0009 and the Army Research Laboratory Materials Center of Excellence through Grant DAAH04-96-2-0006.

References and Notes

(1) Elabd, Y. A.; Sloan, J. M.; Barbari, T. A. *Polymer* **2000**, *41*, 2203.
(2) Maxwell, C. In *Treatise on Electricity and Magnetism*; Oxford University Press: New York, 1873; Vol. 1, p 365.
(3) Rayleigh, L. *Philos. Mag.* **1892**, *34*, 481.
(4) Meridith, R. E.; Tobias, C. W. *J. Electrochem. Soc.* **1961**, *108*, 286.
(5) Prager, S. *Physica* **1963**, *29*, 129.
(6) Neale, G. H.; Nader, W. K. *AIChE J.* **1973**, *19*, 112.
(7) Jeffrey, D. J. *Proc. R. Soc. London* **1973**, *A335*, 355.
(8) Riley, M. R.; Muzzio, F. J.; Buettner, H. M. *AIChE J.* **1995**, *41*, 691.
(9) Fricke, H. *Phys. Rev.* **1924**, *24*, 575.
(10) Hamilton, R. L.; Crosser, O. K. *Ind. Eng. Chem. Fundam.* **1962**, *3*, 187.
(11) Cheng, S. C.; Vachon, R. I. *Int. J. Heat Mass Transfer* **1969**, *12*, 149.
(12) Tsao, G. T. *Ind. Eng. Chem.* **1961**, *53*, 395.
(13) Bell, G. E.; Crank, J. *J. Chem. Soc., Faraday Trans. 2* **1974**, *70*, 1259.
(14) Keller, J. B.; Sachs, D. *J. Appl. Phys.* **1964**, *35*, 537.
(15) Michaels, A. S.; Parker, R. B. *J. Polym. Sci.* **1959**, *41*, 53.
(16) Comyn, J. In *Polymer Permeability*; Elsevier: London, 1985; pp 65−67.
(17) Wakao, N.; Smith, J. M. *Chem. Eng. Sci.* **1962**, *17*, 825.
(18) Weisz, P. B.; Schwartz, A. B. *J. Catal.* **1962**, *1*, 399.
(19) Weissberg, H. L. *J. Appl. Phys.* **1963**, *34*, 2636.
(20) Dullien, F. A. L. In *Porous Media*; Academic Press: New York, 1979; pp 226−227.
(21) Elabd, Y. A.; Barbari, T. A. *AIChE J.* **2001**, *47*, 1255.
(22) Sreenivasan, K. *Polym. J.* **1990**, *22*, 620.
(23) Sreenivasan, K. *J. Macromol. Sci., Phys.* **1993**, *B32*, 125.
(24) Byrne, C. A.; Mack, D. P.; Sloan, J. M. *Rubber Chem. Technol.* **1985**, *58*, 985.
(25) Hong, S. U.; Barbari, T. A.; Sloan, J. M. *J. Polym. Sci., Polym. Phys. Ed.* **1997**, *35*, 1261.
(26) Teo, T. S.; Chen, C. Y.; Kuo, J. F. *Macromolecules* **1997**, *30*, 93.
(27) Senich, G. A.; MacKnight, W. J. *Macromolecules* **1980**, *13*, 106.
(28) Wang, C. B.; Cooper, S. L. *Macromolecules* **1983**, *16*, 775.
(29) Sung, C. S. P.; Schneider, N. S. *J. Mater. Sci.* **1978**, *13*, 1689.
(30) MacKnight, W. J.; Yang, M. *J. Polym. Sci., Part C* **1973**, *42*, 817.
(31) Van Bogart, J. W. C.; Lilaonitkul, A.; Lerner, L. E.; Cooper, S. L. J. *Macromol. Sci. Phys.* **1980**, *B17* (2), 267.
(32) Li, C.; Goodman, S. L.; Albrecht, R. M.; Cooper, S. L. *Macromolecules* **1988**, *21*, 2637.
(33) Seneker, S. D.; Born, L.; Schmelzer, H. G.; Eisenbach, C. D.; Fischer, K. *Colloid Polym. Sci.* **1992**, *270*, 543.
(34) Joseph, M. D.; Savina, M. R.; Harris, R. F. *J. Appl. Polym. Sci.* **1992**, *44*, 1125.

MA002107C